JOURNAL OF CATALYSIS 149, 390–403 (1994)

Investigation of the Reaction Pathways in Selective Catalytic Reduction of NO with NH_3 over V_2O_5 Catalysts: Isotopic Labeling Studies Using $^{18}O_2$, $^{15}NH_3$, ^{15}NO, and $^{15}N^{18}O$[1]

Umit S. Ozkan,[2] Yeping Cai,[3] and Mahesh W. Kumthekar

Department of Chemical Engineering, The Ohio State University, Columbus, Ohio 43210

Received October 19, 1993; revised June 13, 1994

Isotopic tracer studies were performed to investigate the reaction network of selective catalytic reduction of nitric oxide over vanadia catalysts having preferential exposure of different crystal planes. The catalysts were characterized using BET surface area analysis, X-ray diffraction, laser Raman spectroscopy, X-ray photoelectron spectroscopy, scanning electron microscopy, 3-D imaging, and thermal analysis techniques. The product analysis was carried out by a combination of chemiluminescence NO_x analysis, gas chromatography-mass spectrometry, and chemical titration methods. The isotopic labeling experiments were performed under steady-state reaction conditions by using $NH_3 + NO + {}^{16}O_2 \rightarrow NH_3 + NO + {}^{18}O_2$, $^{14}NH_3 + NO + O_2 \rightarrow {}^{15}NH_3 + NO + O_2$, $NH_3 + {}^{14}NO + O_2 \rightarrow NH_3 + {}^{15}NO + O_2$, and $NH_3 + {}^{14}N^{16}O + {}^{16}O_2 \rightarrow NH_3 + {}^{15}N^{18}O + {}^{18}O_2$ switches. Interaction of NO with the vanadia surface was also studied using a $^{14}N^{16}O \rightarrow {}^{15}N^{18}O$ switch. The results obtained in these experiments were combined with the tracer studies performed in ammonia oxidation reactions over the same catalysts to elucidate the reaction pathways involved in SCR reactions, to compare the surface residence times of nitrogen containing species, as well as to quantify the role of ammonia oxidation in SCR reactions. © 1994 Academic Press, Inc.

INTRODUCTION

Selective catalytic reduction (SCR) of nitric oxide has been recognized as a powerful postcombustion pollution control technique to reduce NO_x from stationary sources. Due to the effectiveness of the vanadia-based catalysts to selectively reduce NO with NH_3, and their resistance to SO_2 poisoning, these catalysts have received much attention in recent years (1–11). In spite of the rapidly growing commercial applications for SCR processes and the large number of studies focusing on various aspects of these reactions, there still remain questions about the nature of active sites and the pathway of the SCR reactions over these catalysts.

In our previous studies (12, 13), we demonstrated the structural sensitivity of NO reduction and ammonia oxidation reactions over vanadium pentoxide catalysts and also pointed out the role of ammonia oxidation in determining the selectivity of the SCR reactions. In a more recent article (14), we reported use of an isotopic labeling technique to investigate the mechanisms of oxygen exchange and ammonia oxidation reaction over the unsupported vanadia catalysts with preferential exposure of different crystal planes. The technique employed in this case involves switching from an unlabeled feed mixture to a feed mixture having one or more reactants labeled. This ensures unperturbed steady-state conditions, with the total amount of products remaining constant, while allowing differentiation between different reaction schemes as well as facilitating comparison of surface residence times of various species. That study (14), in addition to confirming that the (010) plane was more active for ammonia oxidation, also demonstrated that the gas phase oxygen actively interacted with the catalyst surface by oxygen exchange. No scrambling of oxygen atoms between the gas phase and the catalyst lattice was observed. It was seen that lattice oxygen tends to diffuse along the direction parallel to the (010) basal plane more readily than in the direction perpendicular to it. It was also found that at least three types of sites were available on the catalyst surface for ammonia adsorption. The V=O sites located on the basal plane were suggested to lead to direct oxidation of ammonia, the actual product formed being a function of the immediate environment on the surface. The surface ammonia species leading to NO formation or to N_2 and N_2O formation through "coupling" were also thought to have different surface residence times.

In the present study, our main focus has been the investigation of the NO interaction with the catalyst surface

[1] Any opinions, findings, and conclusions or recommendations expressed in this publication are those of the authors and do not necessarily reflect the views of the EPA.

[2] To whom correspondence should be addressed.

[3] Present address: Lehigh University, Dept. of Chemical Engineering, Bethlehem, PA 18015.

0021-9517/94 $6.00

and the SCR reactions over V_2O_5 catalysts preferentially exposing different crystal planes. The reaction pathways in the SCR system have been examined through isotopic labeling experiments performed under steady-state conditions using $NH_3 + NO + {}^{16}O_2 \rightarrow NH_3 + NO + {}^{18}O_2$, $^{14}NH_3 + NO + O_2 \rightarrow {}^{15}NH_3 + NO + O_2$, $NH_3 + {}^{14}NO + O_2 \rightarrow NH_3 + {}^{15}NO + O_2$, and $NH_3 + {}^{14}N^{16}O + {}^{16}O_2 \rightarrow NH_3 + {}^{15}N^{18}O + {}^{18}O_2$ switches. The interaction of NO with the surface has been further examined through the $^{14}N^{16}O \rightarrow {}^{15}N^{18}O$ switch. Results from the isotopic labeling studies of ammonia oxidation reactions (14) have been combined with the present results to explain the catalytic trends previously observed over these catalysts.

EXPERIMENTAL

Catalyst Preparation

The preparation of the vanadium pentoxide with preferred exposure of the (010) basal plane and side planes has been described previously (12). The two samples used in this study were prepared by decomposition and calcination of NH_4VO_3 at 520°C for 50 h in a flow of oxygen (V_2O_5-D) and by the temperature-programmed melting and recrystallization (V_2O_5-M). The specific surface areas of V_2O_5-D and V_2O_5-M were 3.4 and 1.0 m^2/g, respectively.

Catalyst Characterization

Catalyst samples were characterized through a number of techniques, including BET surface area measurements, X-ray diffraction, scanning electron microscopy, 3-D imaging technique, X-ray photoelectron spectroscopy, and laser Raman spectroscopy. Adsorption, desorption, and reduction characteristics of the catalysts were also examined through temperature-programmed techniques. Details of the characterization experiments have been presented previously (12).

Reaction Studies

The system used for isotopic labeling studies has been described previously (14). The feed gases consisted of 0.477% NO in He (Linde), 0.53% NH_3 in He (Linde), 10% O_2 in He (Linde), 10% $^{18}O_2$ in He (99 atom% ^{18}O, ICON), 0.5% $^{15}NH_3$ in He (99 atom% ^{15}N, ICON), 0.5% ^{15}NO in He (99 atom% ^{15}N, ICON), 0.5% $^{15}N^{18}O$ in He (99 atom% ^{15}N, 95 atom% ^{18}O, ISOTEC), and pure He (Linde).

The SCR reaction experiments were performed using a feed mixture that consisted of 1500 ppm nitric oxide, 1500 ppm ammonia, and 0.89% oxygen with helium as the balance gas. In nitric oxide exchange experiments, the concentrations of NO and $^{15}N^{18}O$ were maintained at 1500 ppm. The reaction and the exchange experiments were performed at a constant temperature of 400°C. The total volumetric flow rate through the reactor was maintained constant at 100 cm^3(STP)/min. The weight of V_2O_5-D and V_2O_5-M catalysts used were 32 and 66 mg, respectively. The reaction was allowed to reach steady state before a switch was made from an unlabeled gas mixture to a labeled one. Blank reactor runs were also performed over a quartz wool bed. Details of the procedures have been presented elsewhere (14).

Data Analysis

Prior to performing the isotopic switches, fragmentation patterns were obtained for all reaction species, labeled as well as unlabeled, and the relative intensities were recorded for all fragments. These data were later used when correcting for interference from different fragments. All analyses were based on the assumption that the mass spectrometer response of each isotope for any given compound (e.g., ^{14}NO, ^{15}NO) was the same.

The transient for $^{14}NH_3$ was obtained by monitoring the signal for $m/e = 16$. The interference to the $m/e = 16$ signal from oxygen was corrected using the relative intensities of $m/e = 16$ and $m/e = 32$ signals for oxygen that were obtained independently under similar conditions. The transient for $^{15}NH_3$ was obtained by following the $m/e = 17$ signal. The interference from H_2O which has both $m/e = 17$ and $m/e = 18$ signals was corrected by using the relative intensity ratio of these two water fragments. A secondary correction was also used to account for the contribution to the $m/e = 17$ signal from $^{14}NH_3$ which was still in the system.

For all isotopes of N_2O, the molecular ion signals were used. The m/e signals followed were 44 or larger and they did not have any interference from any other species. $^{14}N^{16}O$, $^{15}N^{16}O$, $^{14}N^{18}O$, and $^{15}N^{18}O$ transients were obtained by following the $m/e = 30$, 31, 32, and 33 signals, respectively. The only correction needed was to the $^{14}N^{18}O$ signal for interference from oxygen. The nitrogen isotope transients were obtained by following $m/e = 28$, 29, and 30 signals. The $m/e = 28$ signal was used after the background correction. The $H_2{}^{16}O$ transients were obtained following the $m/e = 18$ signal. Corrections were made for interference from $^{15}NH_3$ or $^{18}O_2$ in those cases where the ammonia or oxygen were labeled. $H_2{}^{18}O$ transient was obtained using $m/e = 20$ signal. The oxygen isotopes $^{16}O_2$, $^{16}O^{18}O$, and $^{18}O_2$ transients were obtained by following the $m/e = 32$, 34, and 36 signals. The normalized concentration of each isotope a given species was calculated by dividing the corrected signal for that isotope by the sum of the signals for all the isotopes of that species.

RESULTS

Catalyst Characterization

Characterization studies, which have been presented in detail previously (12), have demonstrated the preferential

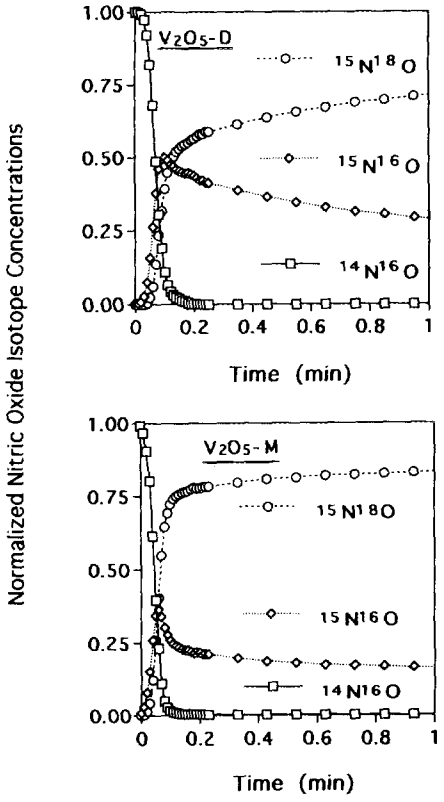

FIG. 1. Normalized nitric oxide isotope concentrations in $^{14}N^{16}O \rightarrow {}^{15}N^{18}O$.

exposure of the (010) basal plane and side planes over the V_2O_5-M and V_2O_5-D catalysts, respectively. It was also shown that the samples with a larger percentage of the (010) plane had a higher relative abundance of the V=O sites exposed. While the steady state activity and selectivity measurements showed the vanadium pentoxide crystals exhibiting catalytic anisotropy in NO reduction and ammonia oxidation reactions, the temperature-programmed techniques pointed out significantly different adsorption, desorption, and reduction characteristics over these catalysts.

Isotopic Labeling Studies

$^{14}N^{16}O \rightarrow {}^{15}N^{18}O$ switch. The oxygen and nitrogen labeling experiments were performed by switching from $^{14}N^{16}O$ to $^{15}N^{18}O$ to examine the oxygen exchange between nitric oxide molecule and the catalyst surface. In these experiments, the nitric oxide concentration was kept at 1500 ppm with He as the balance gas. Transient curves of nitric oxide isotopes from these experiments are illustrated in Fig. 1. Over both catalysts, the $^{14}N^{16}O$ signal fell to zero immediately after the switch. The area under the NO curve equaled to that of Ar relaxation obtained in gas-phase holdup measurements (14), indicating that nitric oxide does not reversibly adsorb on the surface. The $^{15}N^{18}O$ signal, however, did not go up to its inlet concentration immediately. Instead, it quickly rose to an intermediate value and then increased slowly to approach to its inlet level. What was more striking in these transients was the $^{15}N^{16}O$ signal, which showed a sharp increase following the switch and a very slow decay with time, indicating substantial oxygen exchange between catalyst surface and the nitric oxide molecule. Twelve minutes after the switch, 11% of nitric oxide over V_2O_5-D was $^{15}N^{16}O$, while the same percentage over V_2O_5-M was 8%.

The area under the $^{15}N^{16}O$ curve represents the amount of lattice oxygen incorporated into the incoming $^{15}N^{18}O$ molecules. Over the first 12 min, 17% of oxygen in the nitric oxide molecules was replaced by unlabeled oxygen from the catalyst lattice over V_2O_5-D. This number was 11% over V_2O_5-M for the same time period. Another interesting point was that right after the switch, the $^{15}N^{16}O$ signals increased faster over V_2O_5-M than it did over V_2O_5-D. The decay rate of the $^{15}N^{16}O$ signal, immediately following the initial jump, was also seen to be greater over V_2O_5-M than it was over V_2O_5-D.

$NH_3 + NO + {}^{16}O_2 \rightarrow NH_3 + NO + {}^{18}O_2$ switch. The selective catalytic reduction reactions with the switch from unlabeled oxygen to oxygen-18 were carried out over both samples at 400°C. The inlet concentrations of NH_3, NO, and O_2 were maintained at 1500 ppm, 1500 ppm, and 0.89%, respectively, with helium as the balance gas. The transient curves of the oxygen containing prod-

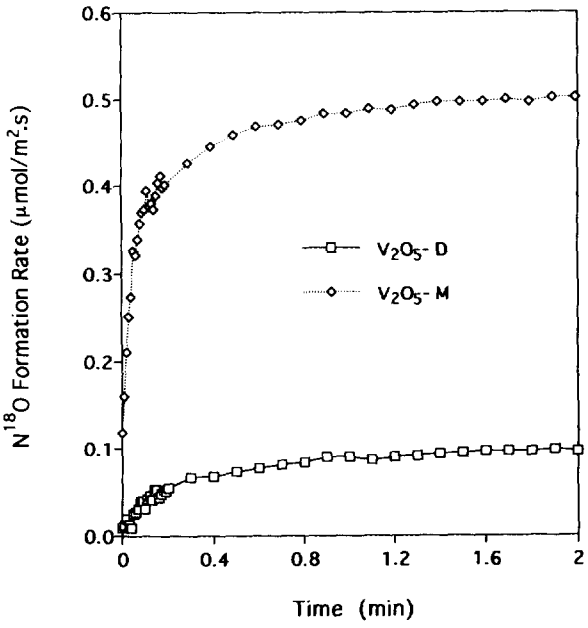

FIG. 2. $N^{18}O$ formation rate in the $NH_3 + NO + {}^{16}O_2 \rightarrow NH_3 + NO + {}^{18}O_2$ switch.

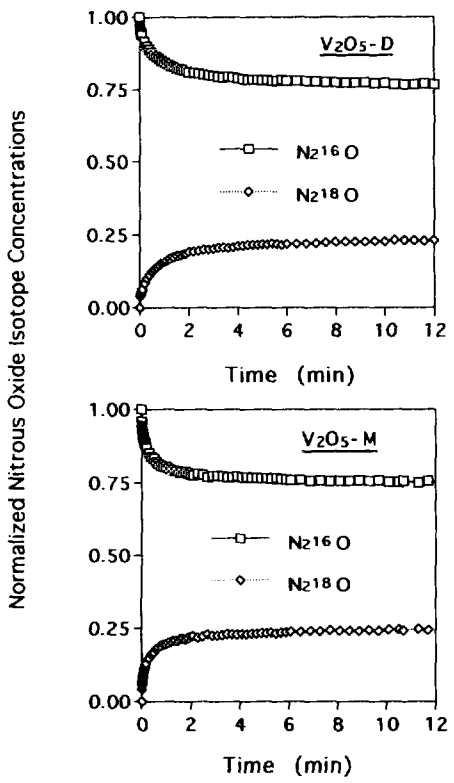

FIG. 3. Normalized nitrous oxide isotope concentrations in the $NH_3 + NO + {}^{16}O_2 \rightarrow NH_3 + NO + {}^{18}O_2$ switch.

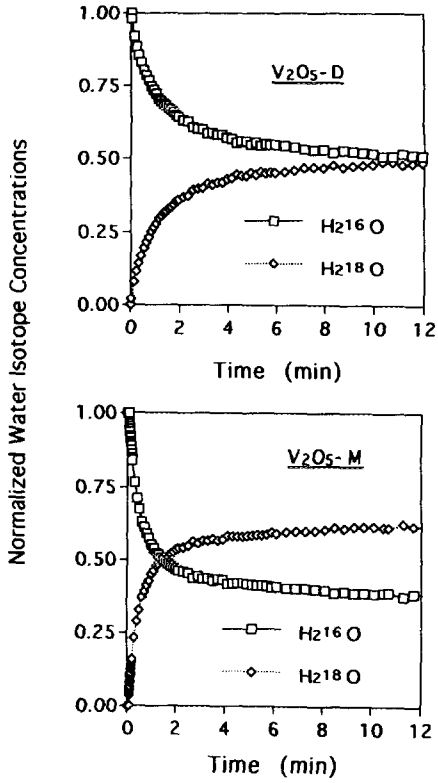

FIG. 4. Normalized water isotope concentrations in the $NH_3 + NO + {}^{16}O_2 \rightarrow NH_3 + NO + {}^{18}O_2$ switch.

ucts are illustrated in Figs. 2–4. The amount of $N^{18}O$ observed at "pseudo-steady state" is an approximate measure of nitric oxide formation via NH_3 oxidation during SCR reaction since the nitric oxide that enters through the feed is unlabeled. In Fig. 2, only $N^{18}O$ transients are shown since NO is a reactant. As found in the ammonia oxidation studies (13, 14), the amount of nitric oxide produced over V_2O_5-D was much smaller in comparison to that over V_2O_5-M. However, the difference between the two catalysts was not as pronounced as it was in the ammonia oxidation reaction.

The transients for nitrous oxide and water isotopes are presented in Figs. 3 and 4. The interesting feature to note in Figs. 3 and 4 is the difference between the oxygen-18 contents of nitrous oxide and water. While both catalysts show less than 25% of nitrous oxide containing labeled oxygen at pseudo-steady state, this percentage is considerably higher in water (50% for V_2O_5-D and 62% for V_2O_5-M). The percentages of unlabeled isotope production are also presented in Table 1. The most striking feature of these results is that the percentage of unlabeled N_2O does not drop very significantly between the first and twelfth minute after the switch. The decrease for the unlabeled water, however, is much more pronounced for both catalysts.

$NH_3 + {}^{14}NO + O_2 \rightarrow NH_3 + {}^{15}NO + O_2$ *switch.* The SCR reactions were also performed using a switch from ^{14}NO to ^{15}NO to examine the formation paths for various nitrogen species. The transient curves of nitric oxide, nitrous oxide, and nitrogen are illustrated in Figs. 5–7. In this case, the unlabeled NO formed after the switch provides a measure of ammonia oxidation leading to nitric oxide formation. In agreement with the previous results, observed NO formation rate over V_2O_5-D is seen to be much lower than it is over V_2O_5-M.

The nitrous oxide transient curves shown in Fig. 6 reveal no doubly labeled nitrous oxide, i.e., $^{15}N_2O$ formation, clearly ruling out the possibility of nitrous oxide

TABLE 1

Percentage (%) of Unlabeled Isotope Production Rates in $NO + NH_3 + {}^{16}O_2 \rightarrow NO + NH_3 + {}^{18}O_2$ Switch

	V_2O_5-D		V_2O_5-M	
	1 min	12 min	1 min	12 min
H_2O	73.5	50.0	56.9	38.0
N_2O	86.1	75.9	84.0	75.1

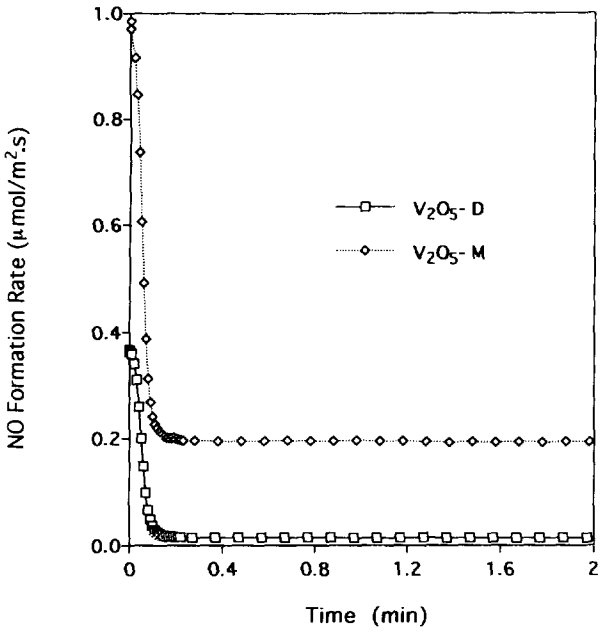

FIG. 5. NO formation rate in the $NH_3 + {}^{14}NO + O_2 \rightarrow NH_3 + {}^{15}NO + O_2$ switch.

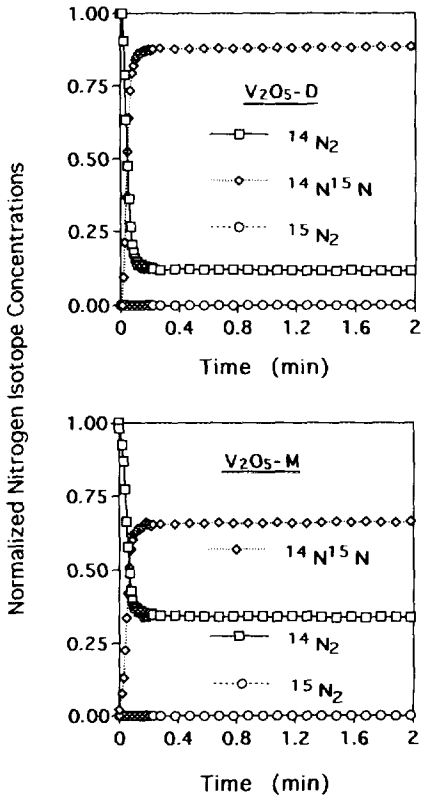

FIG. 7. Normalized nitrogen isotope concentrations in the $NH_3 + {}^{14}NO + O_2 \rightarrow NH_3 + {}^{15}NO + O_2$ switch.

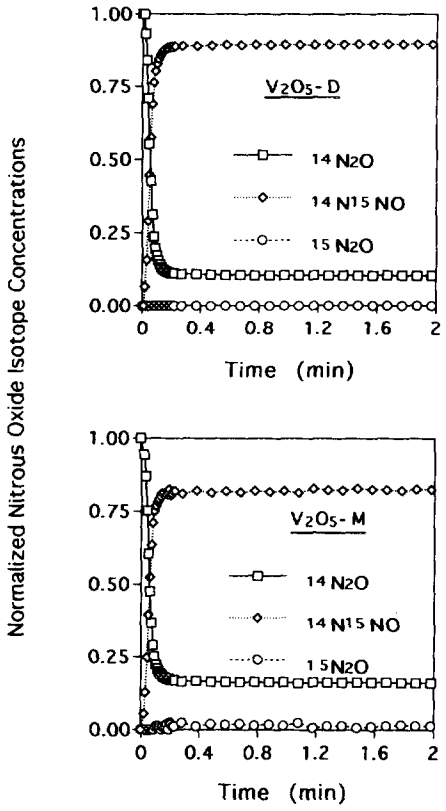

FIG. 6. Normalized nitrous oxide isotope concentrations in the $NH_3 + {}^{14}NO + O_2 \rightarrow NH_3 + {}^{15}NO + O_2$ switch.

formation from two NO molecules. The unlabeled N_2O observed in these experiments is formed through two NH_3 molecules reacting to give nitrous oxide via ammonia oxidation reaction. Based upon the total amount of nitrous oxide produced over a 12 min period, 16% of the N_2O formed over V_2O_5-M and 10% of the N_2O formed over V_2O_5-D are from ammonia oxidation reactions. The remaining nitrous oxide, i.e., 84% over V_2O_5-M and 90% over V_2O_5-D, being in the form of $N^{15}NO$, is produced from one NH_3 molecule reacting with one NO molecule.

The nitrogen transient curves presented in Fig. 7 show no $^{15}N_2$ formation, indicating that a reaction between two NO molecules to give nitrogen is not a viable route in the reaction scheme. Similar to nitrous oxide formation, the unlabeled N_2 is produced from two NH_3 molecules reacting through ammonia oxidation reactions and $N^{15}N$ from one NH_3 molecule reacting with one NO molecule through SCR reactions. The isotope distributions for nitrogen and nitrous oxide are summarized in Table 2. It should be noted that, in this experiment the doubly unlabeled species ($^{14}N_2$ and $^{14}N_2O$) are ammonia oxidation products, whereas cross-labeled species ($^{14}N^{15}N$ and $^{14}N^{15}NO$) result from NO + NH_3 interaction.

$^{14}NH_3 + NO + O_2 \rightarrow {}^{15}NH_3 + NO + O_2$ switch. The

TABLE 2

Percentage (%) of Nitrogen and Nitrous Oxide Isotopes in $^{14}NO + NH_3 + O_2 \rightarrow {}^{15}NO + NH_3 + O_2$ Switch

	N_2	$N^{15}N$	$^{15}N_2$	N_2O	$N^{15}NO$	$^{15}N_2O$
V_2O_5-D	14	86	0	10	90	0
V_2O_5-M	32	68	0	16	84	0

SCR reaction experiments were also performed by switching from unlabeled ammonia to nitrogen-15 labeled ammonia. In this experiment, ^{15}NO can only be produced through direct oxidation of labeled ammonia. The transient curves obtained in this experiment for ^{15}NO are the same as those obtained for ^{14}NO in the $NH_3 + {}^{14}NO + O_2 \rightarrow NH_3 + {}^{15}NO + O_2$ experiments, as expected. Hence, the nitric oxide isotope signals are not presented here.

The three nitrous oxide isotopes observed in this study, N_2O, $N^{15}NO$, and $^{15}N_2O$, are shown in Fig. 8. $N^{15}NO$ is the major form of nitrous oxide over both samples, which is in agreement with the previous reaction with the $NH_3 + {}^{14}NO + O_2 \rightarrow NH_3 + {}^{15}NO + O_2$ switch (Fig. 6). A small amount of unlabeled nitrous oxide is seen to remain after the switch. Since the experiments with the $NH_3 + {}^{14}NO + O_2 \rightarrow NH_3 + {}^{15}NO + O_2$ switch have ruled out the possibility of nitrous oxide formation from two NO molecules, the unlabeled N_2O seen in this experiment has to be produced from two unlabeled ammonia molecules reacting through the ammonia oxidation reaction. The fact that these species are detected even after 2 min following the switch indicates a long surface residence time for ammonia species leading to nitrous oxide formation through direct oxidation. Another point worth noting is that, in Fig. 8, the summation of the $^{14}N_2O$ and $^{15}N_2O$ signals, which result from direct oxidation of ammonia, is not equal to the signal that represents direct ammonia oxidation ($^{14}N_2O$) in Fig. 6. The difference between the two is the amount of cross-labeled nitrous oxide ($^{14}N^{15}NO$) which is formed as a result of direct oxidation of ammonia. This quantity is about 8 and 4.7% of the total nitrous oxide formation over V_2O_5-D and V_2O_5-M, respectively. Also interesting is the fact that the amount of unlabeled nitrous oxide observed in this experiment was much less than that found in ammonia oxidation reaction with the $NH_3 + O_2 \rightarrow {}^{15}NH_3 + O_2$ switch (14). Based on the total amounts of nitrous oxide formed over a period of 2 min, the amounts of N_2O, $N^{15}NO$, and $^{15}N_2O$ are 3, 88, and 9% over V_2O_5-M and 1, 97, and 2% over V_2O_5-D, respectively.

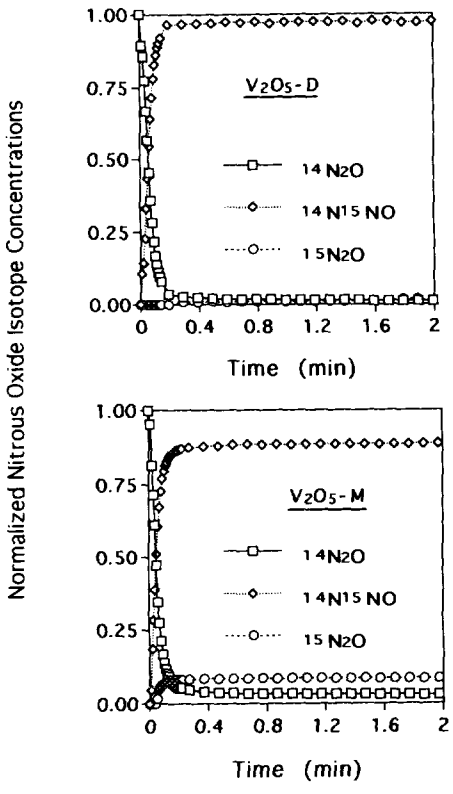

FIG. 8. Normalized nitrous oxide isotope concentrations in the $^{14}NH_3 + NO + O_2 \rightarrow {}^{15}NH_3 + NO + O_2$ switch.

The nitrogen isotope transient curves shown in Fig. 9 reveal that $N^{15}N$ is the major form of nitrogen. This result agrees with the previous findings quite well (Fig. 7). The distributions of different forms of nitrogen over a period of 2 min were found to be 1% of N_2, 58% of $N^{15}N$, and 41% of $^{15}N_2$ over V_2O_5-M. The corresponding values over V_2O_5-D were 4, 76, and 20%. Similar to the formation of nitrous oxide, the small amount of unlabeled nitrogen has to be produced from two adsorbed ammonia species. The amount of the unlabeled N_2 observed in the present experiment was much less than that found in the ammonia oxidation with the $NH_3 + O_2 \rightarrow {}^{15}NH_3 + O_2$ switch (14).

$^{14}N^{16}O + NH_3 + {}^{16}O_2 \rightarrow {}^{15}N^{18}O + NH_3 + {}^{18}O_2$ switch. The SCR reaction network was further studied by labeling the gas phase oxygen, which included both the oxygen in the nitric oxide molecule and the gas-phase molecular oxygen, while also labeling the nitrogen in the nitric oxide. The transient curves for individual nitric oxide isotopes over both V_2O_5-D and V_2O_5-M are illustrated in Fig. 10. The unlabeled NO is the product of ammonia oxidation reaction through incorporation of lattice oxygen. $N^{18}O$, which results from ammonia oxidation reaction using gas-phase oxygen through the surface, increased slowly and reached pseudo-steady state after approximately 10 min over the V_2O_5-M catalyst. Over V_2O_5-D, however, it reached pseudo-steady state almost immediately following the introduction of the labeled gases. The transient curves of $^{15}N^{16}O$ and $^{15}N^{18}O$ resemble

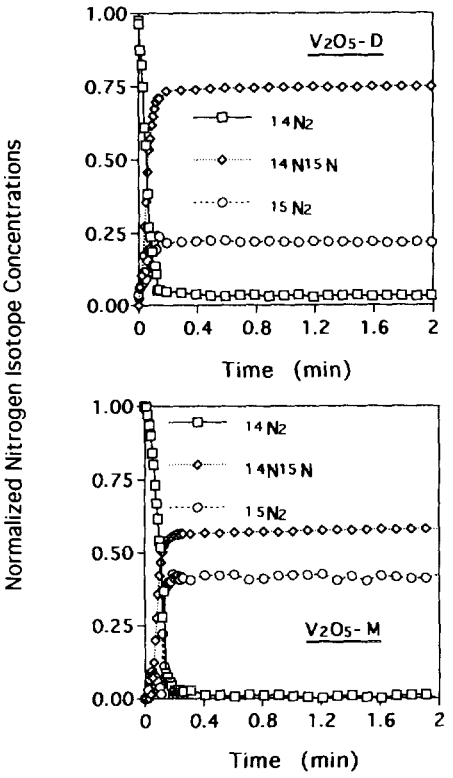

FIG. 9. Normalized nitrogen isotope concentrations in the $^{14}NH_3 + NO + O_2 \rightarrow {}^{15}NH_3 + NO + O_2$ switch.

those in the $^{14}N^{16}O \rightarrow {}^{15}N^{18}O$ switch experiments (Fig. 1), where no gas-phase oxygen was present.

Figure 11 shows the transient curves of unlabeled N-containing species versus labeled ^{15}N-containing species (a and b) and the transient curves of unlabeled oxygen containing species versus ^{18}O-containing species (c and d). The summation of ($NO + N^{18}O$) signals represents the total contribution from the ammonia oxidation reaction leading to the formation of nitric oxide. On the other hand, the ^{15}N-containing species ($^{15}NO + {}^{15}N^{18}O$) are the unreacted nitric oxide remaining in the reaction system. As observed in the ammonia oxidation study (13, 14), the amount of nitric oxide produced from ammonia oxidation reaction is much smaller over V_2O_5-D as compared to that over V_2O_5-M. The trends seen in Fig. 11 agree quite well with those obtained in the previous SCR reaction with $NH_3 + {}^{14}NO + O_2 \rightarrow NH_3 + {}^{15}NO + O_2$ switch (Fig. 5). The O-16 containing nitric oxide results from two different sources, namely ammonia oxidation using lattice oxygen and oxygen exchange between nitric oxide molecule and the catalyst lattice.

The transient curves for individual nitrous oxide isotopes are presented in Fig. 12. Absence of doubly labeled nitrous oxide (i.e., $^{15}N_2O$ or $^{15}N_2{}^{18}O$) in this set of experiments has reiterated the fact that two NO molecules do not couple to give N_2O. The unlabeled N_2O, produced from ammonia oxidation reaction by using lattice oxygen, decreased slowly and disappeared around 4 and 10 min for V_2O_5-D and V_2O_5-M, respectively. $N_2{}^{18}O$, on the other hand, increased and reached a pseudo-steady state. Another interesting feature of these results is the fact that the transient curves of $N^{15}N^{16}O$ and $N^{15}N^{18}O$ show the same trends that were exhibited by $^{15}N^{16}O$ and $^{15}N^{18}O$ transients in the $^{14}N^{16}O \rightarrow {}^{15}N^{18}O$ switch, suggesting that the oxygen inserted into the nitrous oxide molecule comes from nitric oxide molecule and the concentration of oxygen-labeled and oxygen-unlabeled nitrous oxide isotopes is determined by the oxygen exchange between nitric oxide and the surface. The summations of normalized signals from doubly unlabeled N_2-species versus cross-labeled $N^{15}N$-species are shown in Fig. 13 (a and b). Similarly, the summations of the signals from ^{16}O containing species versus ^{18}O containing species are presented in Fig. 13 (c and d). The amount of nitrous oxide produced by ammonia oxidation reaction ($N_2O + N_2{}^{18}O$) over a period of 12 min was found to account for 15% of the total nitrous oxide formed over V_2O_5-M and 10% of that formed over V_2O_5-D. These values are in excellent agreement with those

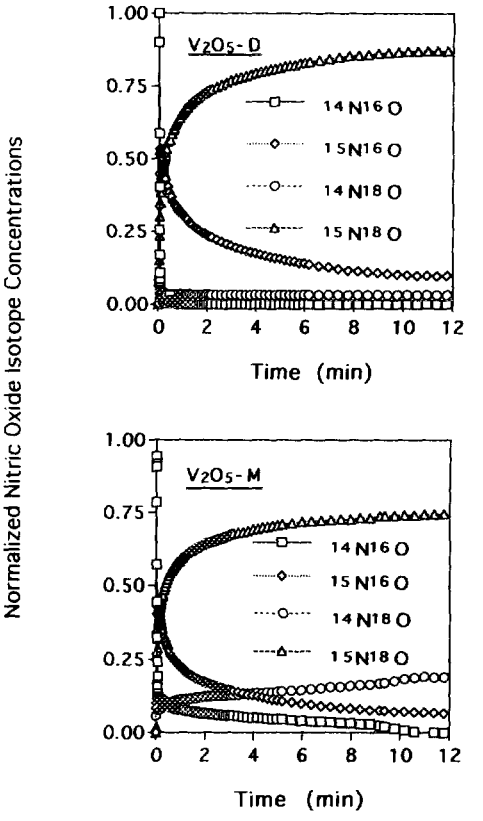

FIG. 10. Normalized nitric oxide isotope concentrations in the $NH_3 + {}^{14}N^{16}O + {}^{16}O_2 \rightarrow NH_3 + {}^{15}N^{18}O + {}^{18}O_2$ switch.

found in the SCR reaction with the switch from [NH_3 + ^{14}NO + O_2] to [NH_3 + ^{15}NO + O_2].

The nitrogen transient signals, which provide a reproducibility check for the previous results, are, as expected, identical to the ones observed following the NH_3 + ^{14}NO + $O_2 \rightarrow NH_3$ + ^{15}NO + O_2 switch (Fig. 7), and therefore, not presented here.

The transient curves for water isotopes are shown in Fig. 14. Comparison of a similar run with only O_2 labeling (Fig. 4) reveals a quick decrease of the H_2O signals accompanied by a fast increase of the $H_2{}^{18}O$ signals. By integrating the area under the curves over a 12-min period, it was found that 23% of water over V_2O_5-M and 32% of water over V_2O_5-D were in the form of unlabeled H_2O. The corresponding data obtained from Fig. 4 were 46 and 69%, respectively.

DISCUSSION

Isotopic labeling studies in SCR reactions described in this paper, when combined with the characterization, thermal analysis, and isotopic labeling studies in ammonia oxidation reactions described previously (12–14), provide important insight into the type of sites and the possible reaction pathways involved in SCR reactions.

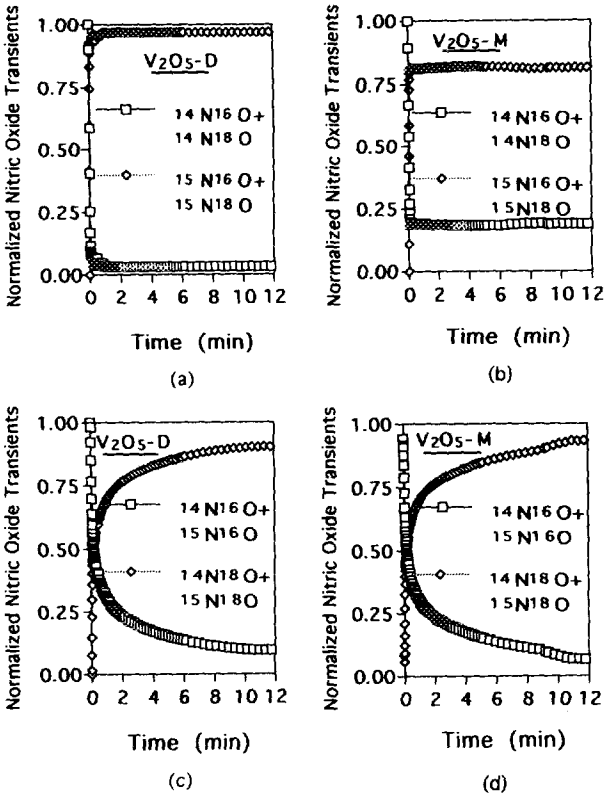

FIG. 11. Comparison of ^{14}N vs ^{15}N and ^{16}O vs ^{18}O isotope concentrations in nitric oxide transients in the NH_3 + $^{14}N^{16}O$ + $^{16}O_2 \rightarrow NH_3$ + $^{15}N^{18}O$ + $^{18}O_2$ switch.

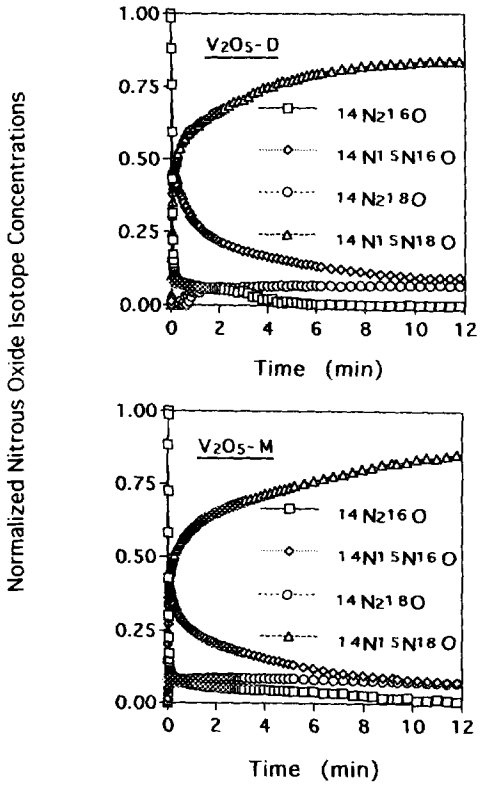

FIG. 12. Normalized nitrous oxide isotope concentrations in the NH_3 + $^{14}N^{16}O$ + $^{16}O_2 \rightarrow NH_3$ + $^{15}N^{18}O$ + $^{18}O_2$ switch.

Characterization studies using SEM, three-dimensional imaging, X-ray diffraction, XPS, and LRS techniques have clearly shown considerable differences in the crystal dimensions for the two catalysts. As a result of the differences in the relative amounts of different crystal planes being exposed on these crystals, there is also a difference in the relative abundance of various sites that are mainly located on a specific plane (e.g., higher abundance of V=O sites over V_2O_5-M).

Interaction of Nitric Oxide with V_2O_5 Surfaces

One of the most interesting findings of this study was the strong interaction between NO molecules and the catalyst lattice in the form of oxygen exchange. This interaction appears to be almost instantaneous, leading to about half of the NO molecules exchanging their oxygen with the catalyst lattice, as seen by the immediate rise in the ^{15}NO signal. Although isotopic labeling studies using nitrogen-labeled nitric oxide does not give any indication of a reversibly adsorbed NO species over V_2O_5 or any appreciable surface residence time for NO, these experiments have clearly indicated the existence of an interac-

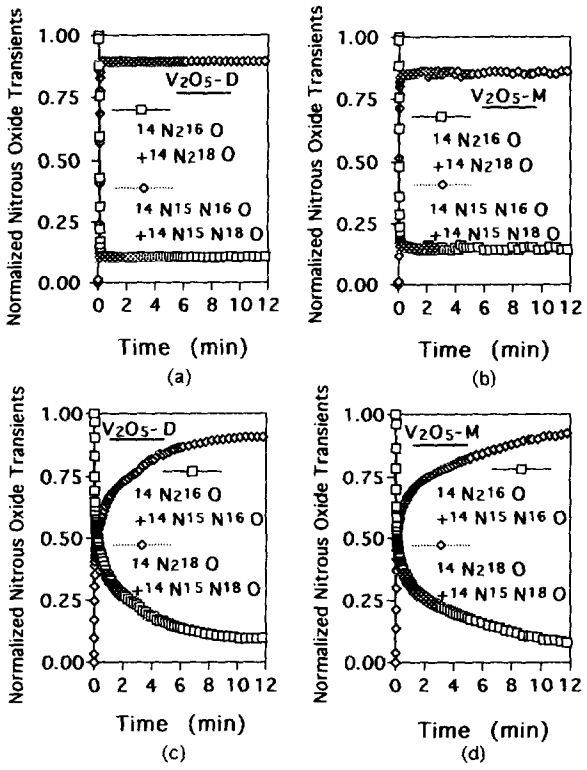

FIG. 13. Comparison of $^{14}N_2$ vs $^{14}N^{15}N$ and ^{16}O vs ^{18}O isotope concentrations in nitrous oxide transients in the $NH_3 + {}^{14}N^{16}O + {}^{16}O_2 \rightarrow NH_3 + {}^{15}N^{18}O + {}^{18}O_2$ switch.

tion, however short-lived it might be, with the surface. Our temperature-programmed adsorption/desorption experiments showed no NO adsorption on the surface, ruling out the possibility of a strongly chemisorbed NO species on the surface. Shelef (15) has observed that the entire oxygen monolayer and even some subsurface oxygen ions can be exchanged at higher temperatures over various metal oxides. He suggested that surface nitrite ions or nitro complexes serve as surface intermediates during the exchange.

Another feature seen through the $^{14}N^{16}O \rightarrow {}^{15}N^{18}O$ switch is that while the slope of the ^{15}NO rise is very steep over V_2O_5-M, once the maximum is reached (Fig. 1), it drops down very rapidly. Over V_2O_5-D, on the other hand, this signal is sustained for a much longer period of time although the initial slope is not as steep as it is over V_2O_5-M. This phenomenon suggests that the surface/subsurface oxygen on the (010) basal plane of V_2O_5-M is very active; however, the rate of the lattice oxygen diffusion to the surface is not as fast as it is over V_2O_5-D. This observation is in agreement with our earlier hydrogen TPR experiments (13) where V_2O_5-M was seen to exhibit a very broad feature at low temperatures, suggesting an easier reducibility of oxygen ions on the (010) basal plane.

As discussed earlier (14), the crystal structure of V_2O_5 reveals sheet-like planes formed along the x–z plane, resulting in an enhanced mobility of the oxygen ions parallel to the (010) plane rather than perpendicular to it. The oxygen diffusion toward the side planes provides a constant ^{16}O source, resulting in more ^{15}NO produced over a span of 12 min over V_2O_5-D than over V_2O_5-M.

Oxygen Labeling Experiments

In the SCR reaction with the switch from $[NH_3 + NO + {}^{16}O_2]$ to $[NH_3 + NO + {}^{18}O_2]$, the amount of $N^{18}O$ produced over V_2O_5-D (0.10 μmol m^{-2} s^{-1}) was less than that over V_2O_5-M (0.5 μmol m^{-2} s^{-1}). The difference, however, was not as pronounced as that found in ammonia oxidation reaction leading to the formation of nitric oxide (14). In this study, it is not possible to attribute all of the $N^{18}O$ formed to the ammonia oxidation reaction. Part of the $N^{18}O$ yield observed could be due to the incoming NO exchanging its oxygen with the lattice as evidenced in the previous $^{14}N^{16}O \rightarrow {}^{15}N^{18}O$ switch experiments. The catalyst surface may have oxygen-18 due to its exchange with molecular gaseous oxygen, as discussed earlier (14). This suggests that the interaction of NO molecule with the lattice oxygen proceeds under the reaction conditions

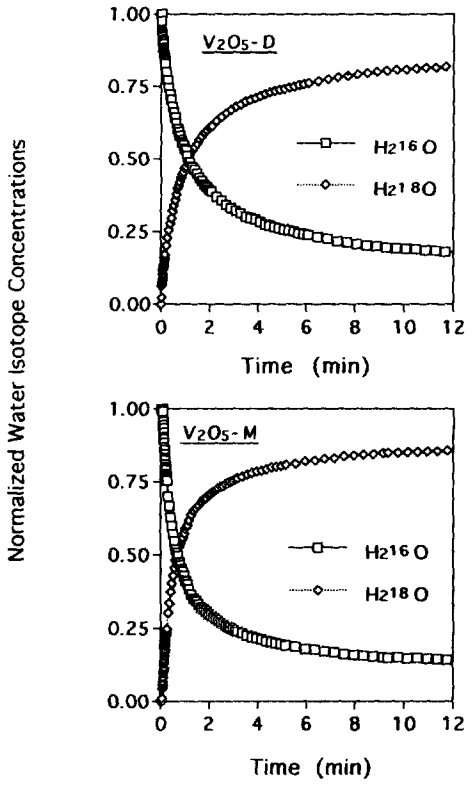

FIG. 14. Normalized water isotope concentrations in the $NH_3 + {}^{14}N^{16}O + {}^{16}O_2 \rightarrow NH_3 + {}^{15}N^{18}O + {}^{18}O_2$ switch.

as well. The direct evidence for the NO-surface interaction under the SCR conditions has been observed in the $NH_3 + {}^{14}N^{16}O + {}^{16}O_2 \rightarrow NH_3 + {}^{15}N^{18}O + {}^{18}O_2$ experiments, where the formation of $^{15}N^{16}O$ was observed immediately after the switch and the concentration of the $^{15}N^{18}O$ rose to its inlet value rather slowly.

The results from the $NH_3 + NO + {}^{16}O_2 \rightarrow NH_3 + NO + {}^{18}O_2$ experiments reveal that the percentage of oxygen-16 containing products over V_2O_5-D was higher than it was over V_2O_5-M. Based on these experiments, however, it is not possible to compare lattice oxygen incorporation into the oxygen-containing products since oxygen-16 could be contributed from NO species as well. The SCR experiments with labeled gaseous oxygen (both NO and O_2), on the other hand, clearly showed a higher percentage of lattice oxygen incorporation into the oxygen-containing products for V_2O_5-D than for V_2O_5-M over a period of 12 min. When the O-16 incorporation rates were compared about 1 min after switch, however, the rate was found to be higher over V_2O_5-M (2.44 μmol m^{-2} s^{-1}) than it was over V_2O_5-D (1.19 μmol m^{-2} s^{-1}), indicating that the surface oxygen on the (010) plane is highly reactive for both exchange and reaction, whereas the diffusion of oxygen towards the (010) plane is not as fast as that parallel to plane. This is in agreement with our earlier findings obtained in the ammonia oxidation reaction (14) as well as in the previous $^{14}N^{16}O \rightarrow {}^{15}N^{18}O$ switch experiments. This phenomenon has been explained by the sheet-like structure of V_2O_5 crystals.

Additional information can be obtained about the source of oxygen when one compares the percentages of unlabeled oxygen in nitrous oxide and water over the two sets of experiments, namely the $NH_3 + NO + O_2 \rightarrow NH_3 + NO + {}^{18}O_2$ and $NH_3 + NO + O_2 \rightarrow NH_3 + {}^{15}N^{18}O + {}^{18}O_2$ switches. In the case of the former (Figs. 3 and 4), the percentage of labeled oxygen in nitrous oxide is much less than the percentage of labeled oxygen in water. In this switch, the behavior observed over the two catalysts is essentially the same for nitrous oxide transients whereas the water transients look considerably different over the two catalysts, with V_2O_5-M giving a higher percentage of labeled water. Also, the percentage of labeled oxygen in nitrous oxide is much lower than the percent of labeled oxygen in water. In the case of the latter switch, however, the percentage of labeled oxygen is about the same in nitrous oxide and water. This observation suggests that oxygen in the nitric oxide molecule gets directly incorporated into the nitrous oxide molecule in the $NO + NH_3$ reaction rather than being used in reoxidation of the surface.

Nitrogen Labeling Experiments

The SCR reaction with the switch from $[NH_3 + {}^{14}NO + O_2]$ to $[NH_3 + {}^{15}NO + O_2]$ showed that the observed NO formation rate from ammonia oxidation reaction is much higher over V_2O_5-M than over V_2O_5-D, agreeing with our earlier findings (14). The most important observation from these experiments is that there was no formation of $^{15}N_2O$ or $^{15}N_2$ over either sample. A similar experiment where the feed mixture was switched from $NH_3 + {}^{14}N^{16}O + {}_{16}O_2 \rightarrow NH_3 + {}^{15}N^{18}O + {}^{18}O_2$ also showed the absence of doubly labeled nitrous oxide and nitrogen ($^{15}N_2O$, $^{15}N_2{}^{18}O$, $^{15}N_2$). This is a clear indication that two molecules of NO do not react to form N_2 or N_2O as suggested by some researchers in the literature (16-18).

In the SCR experiments with labeled NH_3, small amounts of unlabeled N_2 and N_2O were observed over both samples. They are clearly the products of unlabeled NH_3 species lingering on the surface after the switch is made from NH_3 to $^{15}NH_3$ in the gas phase.

Proposed Reaction Scheme

As discussed earlier (14), these studies, combined with our previous investigations, lead us to suggest that ammonia adsorbs on at least three types of sites present on the catalyst surface, which are denoted as types A, B, and C. The type A sites are pairs of V=O centers located on the (010) planes that lead to dissociative adsorption of ammonia to give $V-ONH_2$ and V–OH species. The ammonia species thus created are believed to be short lived, converting quickly to NO and water with an oxygen vacancy and an OH group left behind. The type B sites, which are also located on the (010) planes, are thought to be double-bonded oxygen sites neighboring a V–OH group, leading to the formation of $V-ONH_3$ species. These species appear to have a longer "surface life" and have the ability to couple between themselves to form nitrogen and nitrous oxide or to react with NO to give nitrous oxide. The type C sites are thought to be located mainly on the side planes and to consist of pairs of V–OH groups, leading to the formation of surface ammonium ion species. The structural specificity studies that link nitrogen selectivity in SCR reaction to the side planes lead us to suggest that these are the primary sites that reduce NO selectively. The formations of NO, N_2, and N_2O through ammonia oxidation and through $NO + NH_3$ reaction can be schematized as follows:

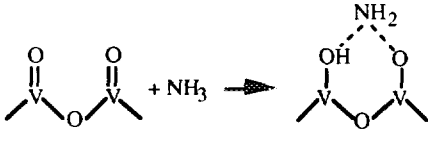

[1]

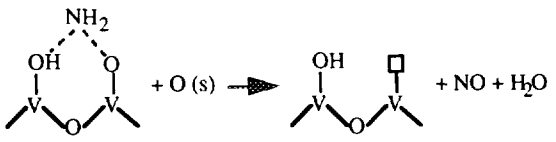

[2]

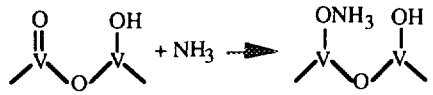

[3]

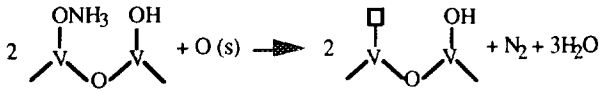

[4]

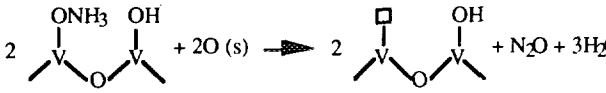

[5]

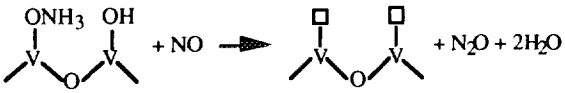

[6]

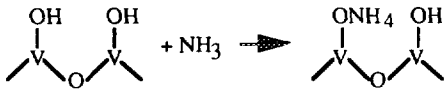

[7]

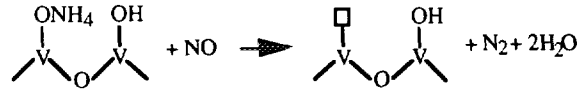

[8]

Although our studies do not provide any information to elucidate the nature of the O species depicted in this network, it is likely that some form of a chemisorbed surface oxygen may be involved in the reaction. Our earlier studies with oxygen exchange experiments (14) lead us to suggest a "four atom surface complex" as described previously by Winter (19), rather than a dissociated species.

Even though it is conceivable that the oxygen vacancies that are left behind can be replenished by both gas phase oxygen and nitric oxide as well as by diffusion of oxygen from the lattice bulk, our results, although not conclusive, suggest that replenishment by NO is not very likely. It appears that the oxygen in NO gets incorporated into N_2O (reaction 6) or into H_2O (reaction 8) directly; however, the replenishment of vacant sites takes place mainly by gas phase oxygen and to a lesser extent by diffusion from the catalyst lattice.

TABLE 3

Percent Contribution of Original Sources of Oxygen in N_2O and H_2O Formation at Pseudo Steady State

	N_2O Formation		H_2O Formation	
	V_2O_5-D (%)	V_2O_5-M (%)	V_2O_5-D (%)	V_2O_5-M (%)
NO	67	66	43	30
Gaseous O_2	24	25	36	56
Bulk O	9	9	21	14

Using nitrogen labeling in SCR reactions not only allows differentiation between different reaction schemes, but it also provides quantitative information about the role of ammonia oxidation in SCR reaction network. While the lack of doubly labeled nitrogen species in $NH_3 + {}^{14}NO + O_2 \rightarrow NH_3 + {}^{15}NO + O_2$ and in $NH_3 + {}^{14}N^{16}O + {}^{16}O_2 \rightarrow NH_3 + {}^{15}N^{18}O + {}^{18}O_2$ switches clearly showed that nitrogen or nitrous oxide formation does not take place through NO–NO interaction, the percentage of doubly unlabeled species in the same experiments provided a direct measure of the extent of ammonia oxidation. The nitrogen-labeling experiments show that over V_2O_5-M, 47% of inlet ammonia is consumed through direct oxidation while this percentage is 24% over V_2O_5-D. These numbers are reproduced through ${}^{15}NO$ labeling, ${}^{15}NH_3$ labeling, and ${}^{15}N^{18}O$ labeling experiments. The structural specificity of both ammonia oxidation and NO + NH_3 reaction has, once again, been demonstrated through isotopic labeling studies.

Another point which should be noted is that although the role of ammonia oxidation in the SCR network has been quantitatively demonstrated in these experiments, the ammonia consumption due to direct oxidation seems to decrease in the presence of NO. One explanation for this could be the possible competition between the coupling of V–ONH_3 species (reactions 4 and 5) and reaction of these species with NO (reaction 6). Another explanation is the hindrance of ammonia adsorption by the interaction of NO molecules with the surface, as seen in ${}^{14}N^{16}O \rightarrow {}^{15}N^{18}O$ switch experiments. The second possibility seems to be more likely, especially for explaining the lower NO formation rates observed when NO is present as a reactant in the feed stream.

A quantitative comparison of the original sources of oxygen incorporated into nitrous oxide and water, based on the combined results of all four sets of isotopic labeling experiments, is presented in Table 3. The values presented in Table 3 do not represent the mechanism with which the oxygen atom gets incorporated into N_2O or

H_2O molecules, but only trace the oxygen contributions back to their original sources before any exchange/interaction took place. Although our results suggest that the oxygen atom in NO molecule gets incorporated into N_2O directly (reaction 6), the O atom in NO molecule itself can originate from different sources. These sources can be the lattice oxygen through an exchange step, as evidenced in the $^{14}N^{16}O \rightarrow {}^{15}N^{18}O$ switch, gas phase oxygen through a "double exchange" step with the lattice oxygen followed by an exchange with NO, and the original O atom in the NO molecule itself. The most striking feature of these percentages is that for nitrous oxide, the contributions of each of the three oxygen sources, i.e., NO, gas phase oxygen, and catalyst lattice, are about the same for the two catalysts. This observation reinforces our suggestion for the type of sites and the reaction steps leading to the formation of N_2O. As seen in the proposed reaction scheme, nitrous oxide formation, both through ammonia oxidation as in reaction 5 and through NO + NH_3 interaction as in reaction 6, takes place mainly on the basal plane. Hence, it is expected that the reactions/interactions leading to N_2O formation should occur to the same relative extent on both catalysts, which results in the same relative contributions from different oxygen sources toward the formation of N_2O.

The fact that the relative extent of the contribution of oxygen from various sources towards the formation of H_2O is different over the two catalysts can also be explained in terms of the proposed reaction network. As seen in reactions 2,4–6, and 8, H_2O is formed in both ammonia oxidation and NO + NH_3 interactions, which involve sites located on both side planes and basal planes. The contribution of oxygen originating from NO which is seen to be higher over V_2O_5-D than it is over V_2O_5-M agrees with our assertion that the side planes (which are preferentially exposed in V_2O_5-D) contains the selective sites for NO + NH_3 interaction leading to N_2 and H_2O formation (reaction 8). Also the fact that the contribution from the catalyst bulk toward the formation of H_2O is higher over V_2O_5-D than over V_2O_5-M can be explained by the faster diffusion rate of oxygen toward the side planes which makes the lattice oxygen from the side planes more readily available as compared to the basal planes.

Comparison of the Present Conclusions with the Mechanisms Proposed Earlier in the Literature

The density of sites available for ammonia adsorption and its role in the reaction system are very important questions that need to be addressed in order to understand the reaction pathway and its mechanism. Although most of the researchers agree that ammonia adsorbs over vanadia-based catalysts, the type of adsorption sites and their nature are quite controversial. One of the earliest mechanisms proposed for the SCR reactions was by Takagi *et al.* (20), who suggested that adsorbed NH_3 was in the form of NH_4^+ species. IR techniques were used to identify the adsorbed species. They also demonstrated the presence of OH groups on the oxidized V_2O_5 surfaces by the water evolving from the surface when the oxide was heated to 650°C. Inomata *et al.* (21) have also suggested that NH_3 was strongly adsorbed on V–OH sites as NH_4^+. Belokopytov *et al.* (22) and Andersson (23, 24) have suggested the presence of Lewis centers on the catalyst surface acting as adsorption sites for electron donating species such as NH_3. Belokopytov *et al.* (22) have correlated the IR bands at 1260 and 1620 cm^{-1} to symmetric and antisymmetric bond vibrations of NH_3 coordinately linked to the surface. Andersson (23, 24) has done crystallographic studies and has concluded that Lewis acid sites exist on the (010) plane in the form of naked V^{5+} ions. Janssen *et al.* (8, 17, 18) proposed the V=O species to the active centers for ammonia activation and suggested that the sites that are easily reduced had a higher activity. They also reported that physically adsorbed ammonia can react with gaseous NO to give the SCR reaction products. It is not clear, however, if physically adsorbed ammonia can still be present on the surface at the reaction temperatures since our previous NH_3 TPD experiments (13) showed the physically adsorbed ammonia desorbing at temperatures as low as 140°C. Gasior *et al.* (25), who investigated the SCR reaction by a pulse technique, suggested that ammonia was adsorbed on the Brønsted sites located on the side planes on the V_2O_5 crystals. More recently, in their detailed study of the titania-supported vanadia system, Went *et al.* (25–27) have concluded that the oxygen atoms participating in the activation of NH_3 are the V=O groups in polyvanadate and monomeric species, the former being more active.

Based on our earlier studies on the structural specificity in ammonia oxidation reactions and in SCR reactions, the ammonia desorption investigations (12–14), as well as the results reported in this paper, we believe that it is not possible to explain the reaction data with only one type of adsorbed species on the surface. It appears that different products of ammonia oxidation and/or NO + NH_3 reaction result from different surface species, as described in the preceding paragraphs. It is quite likely that the three types of adsorbed ammonia species that have been proposed by different researchers, namely V–ONH_2, V–ONH_3, and V–ONH_4 can all be formed over the surface with the type of species formed being controlled by the type of sites and their immediate surface environment. It should also be noted that the oxide surface is highly dynamic in nature under reaction conditions and that it

should be viewed as double-bonded oxygen sites, V–OH sites, and oxygen vacancies being continuously created, used, or interconverted to one another in the presence of water and the gas phase oxygen.

Another point which is still not completely resolved in the literature is whether or not NO adsorbs on vanadia surfaces. Takagi *et al.* (20) suggested that NO adsorbed on the catalyst surface in the form of NO_2(ad). Consequently, the reaction proceeded between NO_2(ad) and adsorbed NH_3 by a Langmuir–Hinshelwood mechanism. Inomato *et al.* (21), on the other hand, proposed that the reaction proceeded between strongly adsorbed NH_3 and gaseous NO by an Eley–Rideal mechanism. Our initial results based on the NO TPD studies (13) suggested that NO is either very weakly adsorbed, or not adsorbed at all, which agreed with the findings by Inomata *et al.* (21) and Gasior *et al.* (25). While the views for NO adsorption over unsupported V_2O_5 catalysts vary significantly, there is also no consensus with regard to NO adsorption over vanadia/titania catalysts. Janssen *et al.* (8, 17, 18) suggested a mechanism in which NO takes part in the SCR reaction as a gas phase species. A similar conclusion was reached by Topsøe (29) who reported no nitric oxide adsorption on fully oxidized or NH_3-reduced vanadia/titania catalysts. Odriozola *et al.* (30) proposed that NO adsorption occurred only on TiO_2 and on reduced V_2O_5, but not on oxidized V_2O_5 surfaces. Although NO was observed over the titania support as a weakly chemisorbed species on Ti^{4+} centers by Ramis *et al.* (31), they concluded that on the ammonia-covered vanadia/titania surfaces, NO is no longer adsorbed over titania and the reaction occurs through the gaseous NO. Went *et al.* (26–28) included an adsorbed NO species in the proposed reaction mechanism although they did not explicitly specify the adsorption sites. The present study demonstrated that NO interacts actively with the catalyst surface, which was also observed by Janssen *et al.* (8, 17, 18). However, this interaction, which leads to significant oxygen exchange between the surface and the NO molecule, appears to be very fast. Therefore, although there is evidence of NO interaction with the surface through oxygen exchange, it is possible that NO does not reside on the surface to react with ammonia and that the SCR reaction proceeds via adsorbed ammonia species reacting with gaseous NO through an Eley–Rideal mechanism.

The role of different oxygen sources (i.e., lattice oxygen, molecular oxygen, and oxygen in NO) is another important question in the SCR reaction scheme. Inomata *et al.* (21) showed that either gaseous oxygen or bulk V=O species can be used to reoxidize the reduced surface V–OH species. Later this suggestion was supported by Gasior *et al.* (25) who showed that in the absence of gas phase oxygen, the reduced surface sites are rapidly regenerated to their initial state by diffusion of oxygen ions from the bulk crystallite, whereas in the presence of gas phase oxygen, the lattice gets more rapidly reoxidized by gaseous O_2. Janssen *et al.* (8, 17, 18) indicated that the surface reoxidation can be brought about by ambient oxygen, by lattice oxygen from underlying layers, or by the oxygen of NO, depending on the reaction conditions. They also stated that the oxygen from the underlying layers on monolayer catalysts does not play an important role in the overall reaction, and the oxygen vacancies are reoxidized more rapidly by O_2 than by NO. In addition to NO and O_2, NO_2 has also been reported as an oxidizing agent (31). General consensus appears to be that the reoxidation with NO is much slower than that with O_2. Also, NO_2 appears to get reduced less effectively than NO under SCR conditions. Our present studies indicate that lattice oxygen is readily used in both ammonia oxidation and SCR reactions and the replenishment of the sites takes place through both gaseous oxygen and diffusion from the catalyst lattice. In the NO + NH_3 reaction, the oxygen in N_2O comes mainly from the NO molecule. Although replenishment of oxygen sites by NO remains as a possibility, we believe most of the reoxidation takes place through molecular oxygen and lattice oxygen and the oxygen in the NO molecules gets directly incorporated into nitrous oxide and/or water.

Another point of controversy in the literature is the question of how nitrogen and nitrous oxide are formed. Although some of the earlier work done using isotopic labeling over supported platinum catalysts suggested that both N atoms in the nitrogen and nitrous oxide molecules came from nitric oxide (16), most of the studies on vanadia-based catalysts showed participation of both nitric oxide and ammonia molecules in the formation of N_2 and N_2O (32, 33). Miyamoto *et al.* (32) reported observing formation of N_2 and N_2O molecules from two NO molecules over V_2O_4 catalysts. Janssen *et al.* (8, 17, 18) suggested the formation of N_2 from two NO molecules during the reoxidation of reduced sites by NO molecules even in the presence of molecular oxygen. However, the N-15 labeling experiments they performed included $^{15}NH_3$, but not ^{15}NO. Our isotopic labeling experiments, especially those that involve N-15 labeled nitric oxide, show that coupling of two NO molecules to form N_2 or N_2O is not a likely step in the reaction scheme. Although reoxidation of the surface with NO in the absence of molecular oxygen cannot be ruled out altogether, it is clear that in the presence of oxygen, reoxidation of the surface takes place through gas phase oxygen and diffusion of oxygen from the subsurface layers.

Direct oxidation of ammonia plays an important role in the SCR reactions, as has been suggested in our earlier studies (13, 14). This study confirms that the activity and selectivity of the SCR reactions cannot be considered alone without investigating the role played by the direct

oxidation of ammonia, especially at temperatures above 300°C. Recently, Odriozola *et al.* (30) reported that NH_3 reduces the vanadium pentoxide surface resulting in the production of N_2O. Janssen *et al.* (8, 17, 18) reported the formation of N_2 from ammonia oxidation reactions, although there was no mention of NO and N_2O formation in their study. In SCR reaction with $^{18}O_2$, Janssen *et al.* (8, 17, 18) attributed the formation of $N^{18}O$ exclusively to the scrambling process. In this study, it is clear that ammonia oxidation, as well as the scrambling process, should be considered as a likely source for $N^{18}O$ formation. Although some reports in the literature indicated observing no product formation from NH_3 interaction with lattice oxygen in NH_3 TPD studies over vanadia catalysts (34), our ammonia TPD studies over V_2O_5 crystals (13) and over 2.3% V_2O_5/TiO_2 (A) catalysts (34) showed NO as well as N_2, N_2O, and H_2O being formed over the surface. Our NH_3 TPD, NH_3 TPR studies as well as direct ammonia oxidation reaction investigations clearly demonstrated that NO as well as N_2 and N_2O can be produced through the direct oxidation of NH_3. The formation of significant quantities of NO during SCR reactions can also explain the observed NH_3 to NO conversion ratios which were much higher than unity (12).

The isotopic labeling studies performed over V_2O_5 samples with preferential exposure of (010) basal plane and side planes have provided important clues about the reaction steps, the nature of sites, and the factors that control selectivity in SCR reactions. The extension of these findings to supported catalysts through TPD, TPR, and isotopic labeling studies over vanadia/titania system is presented in the next paper in this series (35).

ACKNOWLEDGMENTS

This material is based upon the work supported by the Environmental Protection Agency under Award R-815861-01-0. Partial financial support from Exxon Corporation is also gratefully acknowledged.

REFERENCES

1. Bosch, H., Janssen, F. J. J. G., van den Kerkhof, F. M. G., Oldenziel, J., van Ommen, J. G., and Ross, J. R. H., *Appl. Catal.* **25,** 239 (1986).
2. Bauerle, G. L., Wu, S. C., and Nobe, K., *Ind. Eng. Chem. Prod. Res. Dev.* **14**(4), 268 (1975).
3. Bauerle, G. L., Wu, S. C., and Nobe, K., *Ind. Eng. Chem. Prod. Res. Dev.* **17**(2), 117 (1978).
4. Morikawa, S., Yoshida, H., Takahashi, K., and Kurita, S., *Chem. Lett.* 251 (1981).
5. Nam, I-S, Eldridge, J. W., and Kittrell, J. R., *Ind. Eng. Chem. Prod. Res. Dev.* **25**, 186 (1986).
6. Haber, J., Kozlowska, A., and Kozlowski, R., *J. Catal.* **102,** 52 (1986).
7. Inomata, M., Miyamoto, A., Ui, T., Kobayashi, K., and Murakami, Y., *Ind. Eng. Chem. Prod. Res. Dev.* **21,** 424 (1982).
8. Janssen, F. J. J. G., *Kema Sci. Tech. Rep.* **6**(1), 1 (1988).
9. Kotter, M., Lintz, H.-G., Turek, T., and Trimm, D. L., *Appl. Catal.* **52,** 225 (1989).
10. Bond, G. C., and Tahir, S. F., *Appl. Catal.* **71**, 1 (1991).
11. Bosch, H., and Janssen, F., *Catal. Today* **2**, 369 (1988).
12. Ozkan, U. S., Cai, Y., and Kumthekar, M. W., *Appl. Catal. A: General* **96**, 365 (1993).
13. Ozkan, U. S., Cai, Y., Kumthekar, M. W., and Zhang, L., *J. Catal.* **142**, 182 (1993).
14. Ozkan, U. S., Cai, Y., and Kumthekar, M. W., *J. Catal.* **149,** 375 (1994).
15. Shelef, M., *Catal. Rev. Sci. Eng.* **11**(1), 1 (1975).
16. Otto, K., Shelef, M., and Kummer, J. T., *J. Phys. Chem.* **74**(13), 2690 (1970).
17. Janssen, F. J. J. G., van den Kerkhof, M. G., Bosch, H., and Ross, J. R. H., *J. Phys. Chem.* **91**, 5921 (1987).
18. Janssen, F. J. J. G., van den Kerkhof, M. G., Bosch, H., and Ross, J. R. H., *J. Phys. Chem.* **91**, 6633 (1987).
19. Winter, E. R. S., *J. Chem. Soc. A*, 2889 (1968).
20. Takagi, M., Kawai, T., Soma, M., Onish, T., and Tamaru, K., *J. Catal.* **50**, 441 (1977).
21. Inomata, M., Miyamoto, A., and Murakami, Y., *J. Catal.* **62**, 140 (1980).
22. Belokopytov, Y. V., Kholyavenko, K. M., and Gerei, S. V., *J. Catal.* **60**, 1 (1979).
23. Andersson, A. *in* "Adsorption and Catalysis on Oxide Surfaces" (M. Che and G. C. Bond, Eds.), p. 381. Elsevier, Amsterdam, The Netherlands, 1985.
24. Andersson, A., *J. Solid State Chem.* **42**, 263 (1982).
25. Gasior, M., Haber, J., Machej, T., and Czeppe, T., *J. Mol. Catal.* **43**, 359 (1988).
26. Went, G. T., Leu, L.-J., Rosin, R. R., and Bell, A. T., *J. Catal.* **134,** 492 (1992).
27. Went, G. T., Leu, L-J., and Bell, A. T., *J. Catal.* **112,** 479 (1992).
28. Went, G. T., Leu, L-J., Lombardo, S. J., and Bell, A. T., *J. Phys. Chem.* **96,** 2235 (1992).
29. Topsøe, N.-Y., *J. Catal.* **128**, 499 (1991).
30. Odriozola, J. A., Heinemann, H., Somorjai, G. A., Garcia de la Banda, J. F., and Pereira, P., *J. Catal.* **119**, 71 (1989).
31. Ramis, G., Busca, G., Bregani, F., and Forzatti, P., *Appl. Catal.* **64**, 259 (1990).
32. Miyamoto, A., Kobayashi, K., Inomata, M., and Murakami, Y., *J. Phys. Chem.* **86**, 2945 (1982).
33. Takagi, M., Kawai, T., Soma, M., Onishi, T., Tamaru, K., *J. Phys. Chem.* **80**, 430 (1976).
34. Srnak, T. Z., Dumesic, J. A., Clausen, B. S., Tornqvist, E., and Topsøe, N.-Y., *J. Catal.* **135**, 246 (1992).
35. Ozkan, U. S., Cai, Y., and Kumthekar, M. W., submitted for publication.